**RESEARCH ARTICLE**

# Assessment of trends and emission sources of heavy metals from the soil sediments near the Bohai Bay

Kun Liu[1] · Fu Wang[2,3] · Jiwei Li[1] · Shani Tiwari[1] · Bing Chen[1,4]

## Abstract

Anthropogenic emission sources (mainly vehicular and industrial emission) are one of the major emission sources of the heavy metals in aquatic ecosystems which have significant potential to perturb the marine geochemistry and ecosystem as well as human life also. In the present study, we tried to investigate the accumulation of heavy metals (Zn, Cr, Ni, Cu, Pb, Co, As, Cd, and Hg) at two sediment cores near the Bohai Bay in Southern Tianjin and reconstruct their historical trends over the last hundred years to understand the impacts of anthropogenic activities. The concentration of Zn and Cr is found maximum than the other studied heavy metals. Results suggest that in the mid-twentieth century, the maximum concentrations of Zn, Cr, Ni, Cu, and Pb are mainly because of the opening of Dagang Oilfield which emits a huge amount of heavy metals into the environment. Source apportionment analysis has been carried out using positive matrix factorization (PMF) model which suggests three major emission sectors of heavy metals, i.e., coal combustion, manufacturing, and smelting dust, having different contribution 32%, 40%, and 28% respectively to the total heavy metal burden. Industrial emissions are found to be the major sources of Cr, Ni, and Co while Pb is mainly originated from the coal combustion. The risk assessment analysis shows the value of mean effects range median (ERM) quotients ~ 0.17 for the two sediment cores which suggest nearly 21% toxicity of the studied metals indicating towards the policymakers for the mitigation of air pollution surrounding Tianjin.

**Keywords** Sediments · Bohai Bay · Heavy metals · Trends · PMF

✉ Fu Wang
  wfu@cgs.cn

✉ Shani Tiwari
  pshanitiwari@gmail.com

[1] Environmental Research Institute, Shandong University, Qingdao 266237, China

[2] Tianjin Center, China Geological Survey (CGS), Tianjin 300170, China

[3] Key Laboratory of Muddy Coast Geo-environment, China Geological Survey, CGS, Tianjin 300170, China

[4] Laboratory for Marine Geology, Qingdao National Laboratory for Marine Science and Technology, Qingdao 266061, China

## Introduction

During the last few decades, the rapid urbanization/industrialization and economic development of China has led to an increasing trend of heavy metal pollution into the environment (Liu et al. 2019; Peng et al. 2019; Wan et al. 2019; Sun et al. 2018, Tian et al. 2015 and reference therein). Heavy metal is one of the most hazardous pollutants of the environment due to its complex emission sources, toxic nature, and potential for bioaccumulation (Hu et al. 2019; Liu et al. 2019; Hoang et al. 2018; Marchant et al. 2017). They have adverse effects on marine geochemistry, aquatic ecosystem, and fishery industry (Yan et al. 2019; Zhang et al. 2019; Keshavarzi and Kumar 2018). Anthropogenic emission sources such as oil industry, mining, and burning of fossil fuels are recognized as the major sources of heavy metals (Wang et al. 2019; Tian et al. 2015; Chen et al. 2012). They can transport over a large distance from one continent to another through the air, rivers, and oceans (Ming et al. 2019; Wang et al. 2019; Macedo-Miranda et al. 2016, Fang and Chen 2010). They have detrimental impacts on human health

due to access exposure through contaminated foods causing several health diseases like cardiovascular diseases, neurobehavioral disorders, and diabetes. (Sun et al. 2019; Jordanova et al. 2018; Praveena et al. 2015; Li et al. 2014). Mercury (Hg), lead (Pb), arsenic (As), and cadmium (Cd) are the most hazardous among heavy metals and the chronic effects of these heavy metals are well known individually; however, the combined effects of heavy metal on human health are very limited (Khaiwal and Mor 2019; Zhou et al. 2019; Song and Li 2015; Zhang et al. 2015; Li et al. 2014 and reference therein). Earlier, mean concentrations of As, Cd, and Ni in China are reported nearly $51.0 \pm 67.0$, $12.9 \pm 19.6$, $29.0 \pm 39.4$ ng m$^{-3}$ respectively which is quite higher than the upper limit of 6.6, 5, and 25 for World Health Organization (WHO) guidelines (Duan and Tan, 2013). Sediments are a very good indicator of heavy metal pollution from anthropogenic activities due to their hydrophobic nature and tendency to accumulate in sediments as a sink (Liu et al. 2019) and play a crucial role in the transportation of heavy metal in the aquatic system (He et al. 2019; Łuczyńska et al. 2018). Heavy metals in sediments could act as a proxy of the pollution levels and reveal the history of natural and anthropogenic pollution, and hence dating of the sediment is an excellent screening tool to the fingerprint of recent and historical natural and anthropogenic activities (Lin et al. 2017; Grigholm et al. 2016). A recent study found an increasing trend of heavy metals in the sediments over the mainland of China and surrounding oceanic region (Sun et al. 2019; Kang et al. 2018; Tian et al. 2015) which is consistent with the fast economic growth (Chen et al. 2010; Lin et al. 2017). Tian et al. (2015) found an enhancement in heavy metal emission (mainly Hg, Hg, As, Se, Cd, Cr) over China at an annual average growth rate of nearly 5–8% during 1949–2012. On the other hand, the concentration of Zn and Cu decreased by 5–27% in the sediments of Yangtze River during 2005–2016, while a sharp increase in As is also found after 1990 is mainly associated with excessive use of pesticides in agricultural activities (Sun et al. 2019). The contamination levels and distribution of heavy metals are largely influenced by the types of emission sources and their spatial distribution (Yin et al. 2016; Islam et al. 2018). Studies reported that Cu, Zn, Cd, Cr, and Ni were mainly emitted from natural sources while Pb, Cd, As, and Hg from the industrial and agricultural sources (Liu et al. 2019; Zhang et al. 2019; Kang et al. 2018). Thus, the identification of potential emission sources of heavy metals is necessary to investigate the major sectors of environmental pollution. Several methods are used (e.g., principal component analysis (PCA), isotope method, receptor models etc.) to characterize the emission sources and contamination of heavy metals in sediments (Liu et al. 2019; Sun et al. 2019; Huang et al. 2018; Fang et al. 2016; Tian et al. 2015; Gao et al. 2013). PCA method is widely used to characterize the emission sources of pollutants but unable to handle noisy data, resulting in the negative factors loading

(Huang et al. 2018); however, isotope method for source apportionment is quite accurate but relatively more expansive and need a database of the various source samples for references (Gao et al. 2013). On the other hand, potential matrix factorization (PMF) model, an advanced multivariate receptor model, overcomes these limitations and widely used for the source apportionment of environmental pollutants present in atmosphere and water as well as sediment (Liu et al. 2019; Li et al. 2018; Men et al. 2018; Fang et al. 2015; Li et al. 2014). Using PMF model, Liang et al. (2017) found four different emission sectors viz. natural source, atmospheric deposition, industrial activities, and agricultural activities which have different contributions 33.6%, 26.05%, 23.44%, and 16.91% respectively in soil sediments of Lianyuan city, while Liu et al. (2019) found three different emission factors of heavy metal having different contributions in the surface sediments of estuary (Modaomen) in China. Due to the toxic nature, heavy metals are widely used in environmental health risk assessment worldwide through different indices, i.e., geoaccumulation index ($I_{geo}$), potential ecological risk index (PERI), pollution load index (PLI), toxic risk index (TRI), contamination severity index (CSI), and bioavailable metal index (BMI) (Feng et al. 2018; Kumar and Singh 2018; Gao et al. 2018; Zhang et al. 2017; Gusiatin and Kulikowska 2014). The $I_{geo}$ quantify the pollution degree of heavy metals in sediments while PERI provides the toxicity and concentration of heavy metals and can be used to investigate the risk assessment. Using these indices, recently, Zhang et al. (2019) found the pollution level of Cd and Hg relatively higher than the other heavy metals in the surface sediments of Subei Shoal, China, while moderate contamination of heavy metals in the order of Ag > Hg > Se > Sb > As is reported in the sediment of Jinzhou Bay using $I_{geo}$ (Li et al. 2016a).

The coastal region surrounding Bohai Bay is one of the most populated and industrialized areas in the mainland of China and experienced a huge amount of pollutants mainly emitted from Tianjin, Beijing, and Hebei province. Earlier studies in this region found relatively higher Pb and Cd than the standard level and led to an increasing trend of Ni, Cu, and Zn (Ran et al. 2010). The concentrations of As, Pb, Hg, Cu, Ni, Zn, and Cr are found below the environmental quality standard for soils (15, 35, 0.15, 35, 40, 100, and 90 μg/g respectively) in the North China Plain (NCP). However, the concentration of As, Pb, Cu, Ni, Zn, and Cr reached a maximum level in Tianjin province and its surroundings, mainly due to the high density of industrial and mining enterprises and burning of coal for heating in winter (Tan et al. 2011). Although during the last two decades extensive studies of sediments have been carried out over NCP and Bohai Bay for the better understanding of heavy metal pollution, their transportation, emission sources, and potential health/ ecological risk (Liu et al. 2019; Sun et al. 2019; Huang et al.

2018), large uncertainties are still there mainly in their emission sources, and chemical composition of sediments, because of the complex hydrodynamics of river discharge and other atmospheric phenomenon. Thus, more in-depth study on soil sediments with higher accuracy is highly needed which will help to control the anthropogenic activities in the NCP. The main objective of the present study is (1) to determine the concentration of heavy metals, their historical trend during the last century, and impacts of anthropogenic activities; (2) to investigate the potential emission sources of and heavy metal; and (3) to evaluate the risk assessment of heavy metal using mean ERM (effects range median) method. With these objectives, the surface sediments near the Bohai Bay have been analyzed using different techniques which are further described in upcoming sections.

# Materials and methods

## Study area and sample collection

The Bohai Sea is a semi-enclosed sea to the north Yellow Sea, shaped by three marine bays, i.e., Liaodong Bay in the northeast, Laizhou Bay in the south, and Bohai Bay in the west. Bohai Bay covers 15900-km$^2$ area and has a coast of ~ 200 km long with an average water depth ~ 12.5 m, tidal range of 2.4 m surrounded by the deltas of Luanhe and Yellow river from north and south respectively. Along with the coast of the Bay, several small rivers including Hai River and Duliujian River also enter into the Bay through the Tianjin new port near Tanggu. The industrial pollution mainly dominated by petrochemicals and metallurgical industries is highly toxic and discharged into the Bay through the rivers. In this region, at two salt-marsh sites, S4 and S5 (Fig. 1), and sediment samples are collected from the sidewall of the 1-m-deep pit at every 1-cm interval. The detail of the sampling location is given in Table 1. The collected samples are kept in an airtight bag and kept at ~ 4° C until analysis.

## Analytical methods

### Geochronology

In the laboratory, subsamples are grounded after being dried and stored in an airtight box for more than 1 month to ensure the equilibrium between $^{226}$Ra and its daughter $^{222}$Rn (half-life of 3.8 days). The activities of total $^{210}$Pb, $^{137}$Cs, and $^{226}$Ra (by way of its granddaughter $^{214}$Pb) are measured using gamma spectrometry based on the photon energies at 46.5, 662, and 295 + 352 keV, respectively. $^{210}$Pb$_{exc}$ for each sample is calculated by subtracting $^{226}$Ra ($^{214}$Pb) from the total $^{210}$Pb (Bq kg$^{-1}$) measured. The measurements have been carried out using a detector (GWL-120-15, ORTEC) installed at the

Nanjing Institute of Geography and Limnology, Chinese Academy of Sciences (NIGL, CAS), which is well calibrated by radioisotope standards from the Environmental Radioactivity Research Center of University of Liverpool and China Institute of Atomic Energy. An age model, constant initial concentration (CIC), is used to calculate the age of sediment and the observed uncertainty is found within the ± 4 years.

## Chemical analysis

Cupper (Cu), cobalt (Co), chromium (Cr), nickel (Ni), zinc (Zn), cadmium (Cd), and lead (Pb) of sediment samples are measured with an inductively coupled plasma mass spectrometry (ICP-MS, X Siereis, America). 0.1 g sample is dissolved in ultra-pure HNO$_3$/HClO$_4$/HF to digest the sediments and remain heavy metals in the residues (Li et al. 2000). Then the electro-thermal board is used to heat and resolve the sample. After heating, (1 + 1) HNO$_3$ 10 mL is used to resolve the residue. Such demineralization sediments are diluted in 200 mL of water and measured with the ICP-MS which is calibrated with an external standard.

An atomic fluorescence spectrometry (AFS, AFS-933, China) is used to determinate As and Hg in the sediments. 0.5 g sample was put in a 25 mL colorimetric tube. Ten milliliters (1 + 1) of aqua regia is added to the tube, which is used to digest all remaining metals in the residue. After, that tube is heated in boiling water for 1 h. After heating, 1 mL potassium permanganate (1%) is used to digest the residue and dilute with oxalic acid (1%) to 25 mL. Four different Chinese geochemical standard references, i.e., GSD5a, GCD-16, GSS13, and GSS-19, are used to control the analytical quality. The 20% of the total samples (i.e., 12 out of 60 samples) are tested in duplicate and the average relative standard deviation is found around 4%. The average difference in standard and observed values is found by nearly 8%.

## Loss of ignition measurement

The loss of ignition (LOI) is a very popular, fast, inexpensive, and widely used method to estimate the organic and carbonate component in sediments (Dai et al. 2019; Chen et al. 2018; Ghosh and Maiti 2018). In this method, accurate 1 g of sample is placed into a high-temperature furnace and burnt at 950–1000° C for 15–20 min and weighed it for the calculation of the LOI. The LOI of the sample is given by:

$$\text{LOI } (\%) = (G_1 - G_2)/G_1 \times 100 \qquad (1)$$

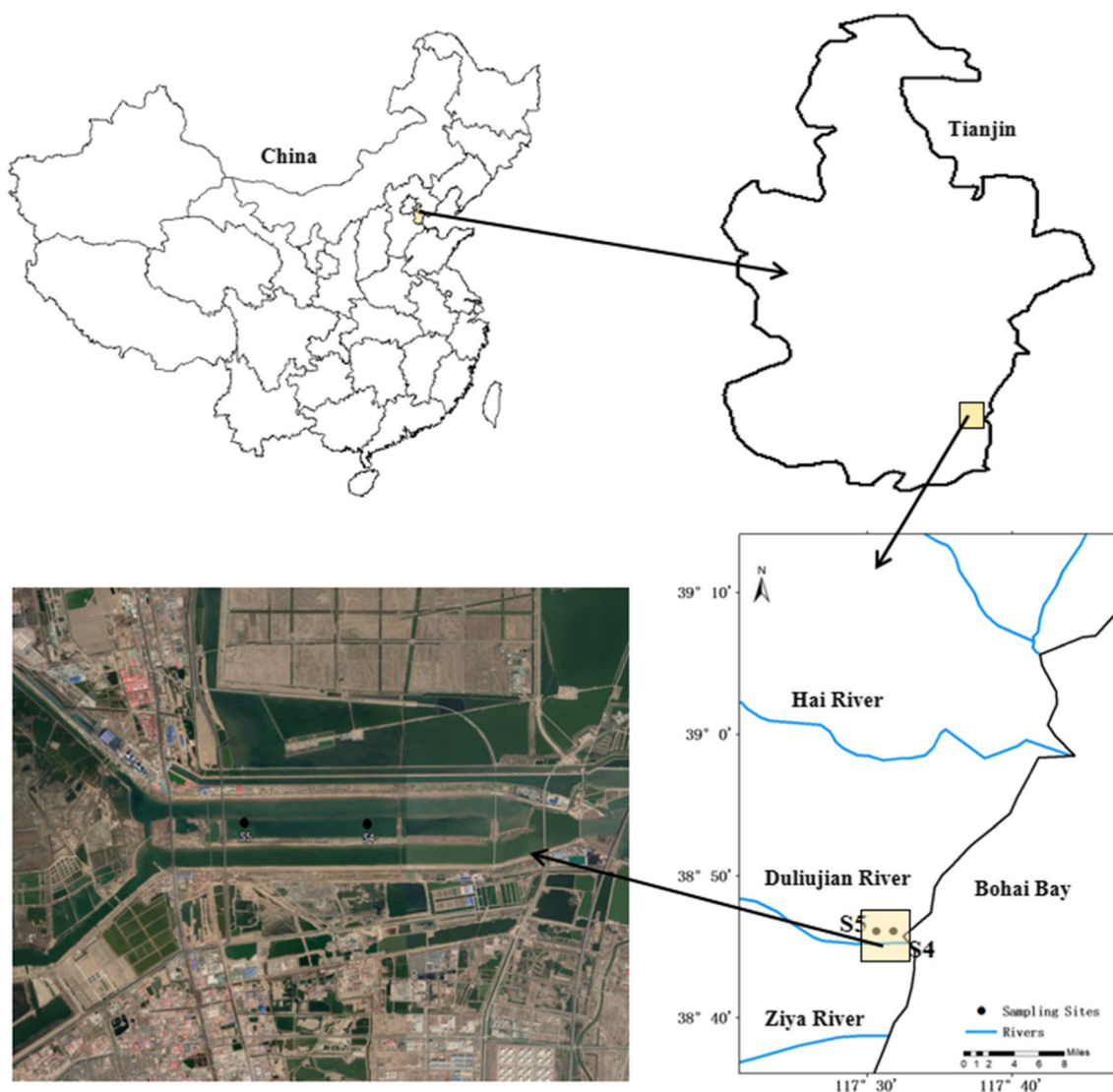where $G_1$ and $G_2$ are the mass of the sample before and after burning respectively.

**Fig. 1** Location map and sampling sites

## Positive matrix factorization model

We used a positive matrix factorization (PMF) model to resolve the major sources of heavy metals. It is a bilinear receptor model and based on the following equation:

$$xij = \sum_{k=1}^{p} g_{ik}f_{kj} + e_{ij} \qquad (2)$$

where $x_{ij}$ is the concentration of $j$ species obtained on $i$ sample, $p$ is the number of factors, $g_{ik}$ is the contribution of factor $k$ on sample $i$, $f_{kj}$ is the concentration of species $j$ in factor $k$, and $e_{ij}$

is the error of this model for the $j$ species measured on $i$ sample. It can be used as source apportionment without source file information (Fang et al. 2016; Lin et al. 2011; Hopke, 1991). PMF model is based on the inherent correlation between observed data and analyses of the main contributing emission factors of heavy metals. The object function ($Q$) is the weighted sum of squares of differences between the PMF output and the original data set and used to estimate the stability of the model. One of the main objectives of PMF analysis is to minimize the $Q$ value. Further details about the PMF model is discussed elsewhere (Li et al. 2018). In the present study, Environmental Protection Agency—EPA PMF 5.0

**Table 1** Sampling information of sediment cores

| Code | Location | Sub environment | Description |
|------|----------|-----------------|-------------|
| S4 | 38° 46′ 05.5″ N, 117° 31′ 50.0″ E | Salt marsh | 1.0 m long, yellowish brown clayey silt |
| S5 | 38° 46′ 05.3″ N, 117° 30′ 38.8″ E | Salt marsh | 1.0 m long, yellowish brown clayey silt |

model software—approved by the US Environmental Protection Agency is used to simulate the concentration of nine heavy metals (Cu, Pb, Zn, Cr, Ni, Co, Cd, Hg, and As) at sites S4 and S5. In the process of PMF simulation, in order to select the optimal number of factors, 2 to 5 factors are examined. The model has been run for 20 times with a random seed to determine the stability of $Q$ values (Kara et al. 2015). The variability in the PMF solution is estimated by error estimation (EE) diagnostics and summarized in Table S3 and S4. The value of $Q$robust/$Q$exp decrease and reached from 0.426 to 0.177 as we increase the number of factors from 2 to 5. In the present study, the optimal 3-factor solution was selected for the PMF analysis. Once the optimal solution of factor is obtained, the rotational ambiguity is handled using the $F_{peak}$ parameter (0.1, 0.5, − 0.5, 1, − 1) to explore alternative solutions by estimating the variation of the $Q$ values. The correlation between measured and PMF simulated concentrations was significant ($R^2 = 0.93$). In the present study, the uncertainty about 20% is adopted based on the results from earlier work (Li et al. 2018; Lin et al. 2011).

### Time series trend analysis

A Mann–Kendall test has been applied to detect whether the trends in species are statistically significant (Hirsch et al. 1982). The trend test is a non-parametric test that has been proved to be applicable for those data which does not have normal distribution due to having low sensitivity to abrupt breaks (Carslaw 2005). It is recommended by the World Meteorological Organization (WMO) for public application and widely used in evaluation of trend in climatic, hydrological, and water resources data set (Tian et al. 2015, Maes et al. 2018; Montanher et al. 2018; Rahman et al. 2018; Jaiswal et al. 2015). In the present study, the time series of chemical species are tested and statistical parameters, i.e., mean and standard deviation (STD), are calculated for normal distribution while median and median absolute deviation (MAD) is calculated for non-normal distribution.

## Results and discussion

### Sediment properties

The LOI for both sediment core (S4 and S5) as a function of depth (cm) is shown in Fig. 2. A relatively higher value of LOI is observed for core S5 than S4, suggesting the higher concentration of organic matter at S5 which may be mainly due to larger deposition of pollutants through the river discharge. The figure also reveals a constant LOI value before 6.5 cm depth and then after it increases abruptly at both S4 and S5 cores. The increase in LOI in the upper layer of sediments may suggest faster deposition of organic matter through the anthropogenic activities. Recent studies also found a higher
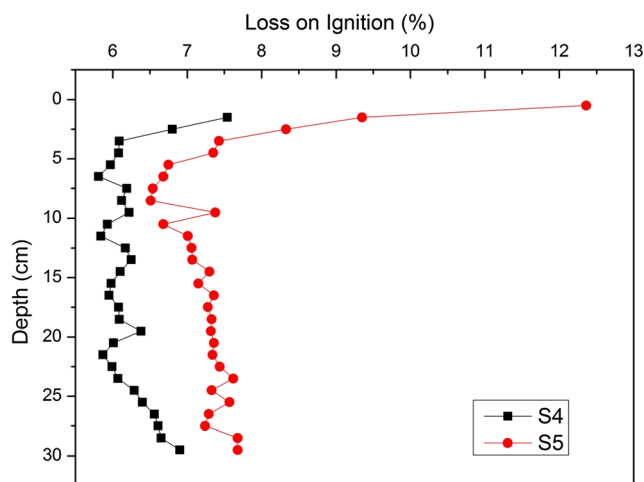


**Fig. 2** Sediment core loss on ignition in S4 and S5

concentration of organic matter in the sediment of Bohai Sea, Yellow Sea, and East China Sea (Ji et al. 2019; Chen et al. 2018; Fang et al. 2018). A close correlation between the loss on ignition (LOI) of lake sediments with the organic matter and carbonate of the sediments is also reported by earlier researchers (Ziting et al. 2006). The age of the sediments for both core sites (S4 and S5) are given in Table 2 which reflect a little difference in ages. The sediment's age is also well correlated with LOI which indicates that the drastic increase in LOI since the early 1990s that may be mainly because of the rapid increase in anthropogenic activities

**Table 2** Geochronology of cores S4 and S5

| Depth (cm) | Year | |
|---|---|---|
| | S4 | S5 |
| 0–1 | 2011 | 2010 |
| 1–2 | 2008 | 2006 |
| 2–3 | 2004 | 2002 |
| 3–4 | 1999 | 2000 |
| 4–5 | 1996 | 1998 |
| 5–6 | 1992 | 1995 |
| 6–7 | 1987 | 1991 |
| 7–8 | 1982 | 1986 |
| 8–9 | 1978 | 1980 |
| 9–10 | 1977 | 1976 |
| 10–11 | 1974 | 1974 |
| 11–12 | 1969 | 1973 |
| 12–13 | 1967 | 1970 |
| 13–14 | 1962 | 1963 |
| 14–15 | 1952 | 1954 |
| 15–16 | 1940 | 1941 |
| 16–17 | 1935 | 1930 |
| 17–18 | 1925 | 1909 |

(mostly from the industry and transportation) in the NCP and will be further discussed in the upcoming section. A large increase in organic matter deposition since 1990 is also reported in sediments of Chaohu and Taihu lakes (Han et al. 2011) in Southern China, in Eastern China Marginal Seas (Fang et al. 2018), in Sanjiang Plain (Gao et al. 2014), in the remote lake Qinghai (Han 2015), and in the Nam Co Lake (Cong et al. 2013) in the Tibetan Plateau.

## Heavy metal concentrations and their trends

The concentrations of heavy metals as a function of depth (cm) are summarized in Table 3 and Table 4 along with their average (AVG), standard deviation (STD), median,

and median absolute deviation (MAD) for the core sites S4 and S5, respectively. As shown in the table, the mean concentrations of heavy metals in sediments of S4 are as follows: 33.82 µg g$^{-1}$ for Cu, 23.81 µg g$^{-1}$ for Pb, 75.02 µg g$^{-1}$ for Zn, 66.37 µg g$^{-1}$ for Cr, 29.01 µg g$^{-1}$ for Ni, 11.70 µg g$^{-1}$ for Co, 0.17 µg g$^{-1}$ for Cd, 10.53 µg g$^{-1}$ As, and 0.02 µg g$^{-1}$ for Hg respectively which are in the order of Zn > Cr > Cu > Ni > Pb > Co > As > Cd > Hg to their concentrations. On the other hand, the mean concentrations of heavy metals for sediments of site S5 are as follows: 27.97 µg g$^{-1}$ for Cu, 24.24 µg g$^{-1}$ for Pb, 77.87 µg g$^{-1}$ for Zn, 64.63 µg g$^{-1}$ for Cr, 30.21 µg g$^{-1}$ for Ni, 12.13 µg g$^{-1}$ for Co, 0.15 µg g$^{-1}$ for Cd, 11.24 µg g$^{-1}$ for As, and 0.02 µg g$^{-1}$ for Hg respectively which are

**Table 3** Heavy metal concentrations at core S4 (µg g$^{-1}$)

| Depth (cm) | Cu | Pb | Zn | Cr | Ni | Co | Cd | As | Hg |
|---|---|---|---|---|---|---|---|---|---|
| 0–1 | 28.3 | 25.7 | 96.7 | 61.2 | 28.8 | 10.6 | 0.15 | 8.65 | 0.023 |
| 1–2 | 30.7 | 26.5 | 102 | 64 | 31.6 | 11.7 | 0.13 | 11.2 | 0.029 |
| 2–3 | 28.8 | 31.2 | 88.9 | 68.4 | 31.1 | 12.2 | 0.12 | 11.9 | 0.022 |
| 3–4 | 28.9 | 21.5 | 75.6 | 63.7 | 28.2 | 11.5 | 0.12 | 11.1 | 0.026 |
| 4–5 | 29.2 | 26.9 | 75.4 | 63.8 | 27.7 | 11.4 | 0.15 | 10.6 | 0.014 |
| 5–6 | 32.8 | 35.8 | 75.8 | 63.6 | 27.8 | 11.7 | 0.15 | 10.4 | 0.016 |
| 6–7 | 34.2 | 21 | 71.2 | 65.1 | 28.1 | 11.6 | 0.2 | 10.4 | 0.014 |
| 7–8 | 33.9 | 24.5 | 74.1 | 68.9 | 30 | 12.2 | 0.24 | 11 | 0.015 |
| 8–9 | 34.9 | 24.5 | 70.5 | 68.3 | 29.7 | 11.8 | 0.22 | 9.83 | 0.046 |
| 9–10 | 43.5 | 22.8 | 82.8 | 68.4 | 29.8 | 12.2 | 0.16 | 11.2 | 0.021 |
| 10–11 | 51 | 26.6 | 83.3 | 71.5 | 29.4 | 11.8 | 0.21 | 9.81 | 0.016 |
| 11–12 | 48.2 | 21.3 | 76.5 | 71.3 | 29.6 | 12.2 | 0.12 | 10.1 | 0.015 |
| 12–13 | 39.4 | 20.4 | 74.8 | 69.6 | 29.3 | 12 | 0.15 | 10.5 | 0.022 |
| 13–14 | 38.1 | 25.5 | 76.7 | 68.9 | 29.6 | 11.9 | 0.2 | 11.1 | 0.016 |
| 14–15 | 36.6 | 22 | 76.9 | 67.2 | 28.6 | 11.7 | 0.18 | 10.8 | 0.018 |
| 15–16 | 36 | 23.1 | 72.9 | 66.2 | 29.8 | 11.8 | 0.19 | 11.2 | 0.017 |
| 16–17 | 31.6 | 22.3 | 68.9 | 67.6 | 28.6 | 11.6 | 0.19 | 10.9 | 0.053 |
| 17–18 | 34.1 | 25.8 | 74.1 | 67.2 | 29.5 | 11.9 | 0.22 | 10.5 | 0.016 |
| 18–19 | 31.8 | 24.6 | 73.8 | 65.3 | 28.7 | 11.5 | 0.2 | 8.98 | 0.013 |
| 19–20 | 33.2 | 21.9 | 67 | 67.8 | 28.6 | 11.7 | 0.18 | 10.6 | 0.015 |
| 20–21 | 30.1 | 26.2 | 66.8 | 67.7 | 27.9 | 11.3 | 0.19 | 9.39 | 0.012 |
| 21–22 | 31.2 | 19.9 | 66.4 | 65.7 | 27.2 | 11.2 | 0.16 | 9.74 | 0.012 |
| 22–23 | 30 | 22.2 | 67.1 | 66.8 | 28.4 | 11.4 | 0.12 | 9.99 | 0.012 |
| 23–24 | 31.4 | 17.7 | 67.6 | 63.5 | 27.5 | 11.2 | 0.13 | 10.2 | 0.014 |
| 24–25 | 27.9 | 20.2 | 65 | 62.6 | 27 | 11.3 | 0.14 | 10.1 | 0.015 |
| 25–26 | 31.1 | 21.2 | 70.7 | 64.4 | 28.7 | 11.5 | 0.16 | 10.7 | 0.013 |
| 26–27 | 32.4 | 23.2 | 70.4 | 65.5 | 29.9 | 11.9 | 0.19 | 11.1 | 0.012 |
| 27–28 | 34.8 | 21.4 | 70.2 | 66.4 | 29.9 | 12.1 | 0.15 | 11.4 | 0.012 |
| 28–29 | 32.3 | 27.7 | 75.5 | 65.9 | 30 | 12.2 | 0.19 | 11.4 | 0.012 |
| 29–30 | 28.2 | 20.6 | 72.9 | 64.7 | 29.3 | 12 | 0.15 | 11.2 | 0.016 |
| Mean | 33.82 | 23.81 | 75.02 | 66.37 | 29.01 | 11.70 | 0.17 | 10.53 | 0.02 |
| STD | 5.57 | 3.66 | 8.51 | 2.49 | 1.09 | 0.38 | 0.03 | 0.75 | 0.01 |
| Median | 32.35 | 22.95 | 73.95 | 66.3 | 29.05 | 11.7 | 0.16 | 10.6 | 0.0155 |
| MAD | 2.40 | 2.15 | 3.35 | 1.95 | 0.75 | 0.25 | 0.03 | 0.50 | 0.0025 |

**Table 4** Heavy metal concentrations at core S5 (µg g$^{-1}$)

| Depth (cm) | Cu | Pb | Zn | Cr | Ni | Co | Cd | As | Hg |
|---|---|---|---|---|---|---|---|---|---|
| 0–1 | 26.4 | 33.2 | 123 | 67.6 | 35 | 11.2 | 0.25 | 10.5 | 0.031 |
| 1–2 | 25.4 | 34.2 | 105 | 64.6 | 33.8 | 11.9 | 0.14 | 11.3 | 0.027 |
| 2–3 | 25.7 | 34.6 | 91.7 | 65.8 | 34.3 | 12.6 | 0.12 | 11.7 | 0.039 |
| 3–4 | 29.5 | 28.5 | 87.2 | 66 | 32.9 | 12.3 | 0.12 | 12.8 | 0.022 |
| 4–5 | 32.5 | 26.5 | 82.9 | 66.1 | 31 | 12.3 | 0.16 | 12 | 0.016 |
| 5–6 | 28.5 | 24.9 | 76.8 | 65.1 | 29.9 | 12.2 | 0.18 | 11.8 | 0.016 |
| 6–7 | 26.7 | 23.9 | 70.8 | 65.5 | 30.2 | 12.4 | 0.17 | 11.6 | 0.013 |
| 7–8 | 28.4 | 25.1 | 72.3 | 65.9 | 29.6 | 12.2 | 0.17 | 12 | 0.013 |
| 8–9 | 26.5 | 25.1 | 79.1 | 66 | 30.2 | 12.3 | 0.2 | 11.5 | 0.013 |
| 9–10 | 30.8 | 22.6 | 78.4 | 65.9 | 30.5 | 12.4 | 0.14 | 11.9 | 0.02 |
| 10–11 | 28.5 | 26.7 | 78.8 | 64.5 | 29 | 11.8 | 0.26 | 10.7 | 0.016 |
| 11–12 | 29.5 | 22.8 | 73.6 | 65 | 29.1 | 12 | 0.16 | 10 | 0.016 |
| 12–13 | 29.1 | 21.7 | 78.4 | 66.9 | 29.4 | 12.1 | 0.13 | 10.8 | 0.016 |
| 13–14 | 24.6 | 19.7 | 71 | 64.2 | 28.7 | 11.9 | 0.12 | 10.6 | 0.013 |
| 14–15 | 27.4 | 22 | 75 | 63.4 | 29.4 | 12 | 0.14 | 10.6 | 0.017 |
| 15–16 | 28.5 | 22.2 | 72.1 | 63.2 | 28.6 | 11.9 | 0.15 | 11 | 0.018 |
| 16–17 | 26 | 21.6 | 69.2 | 66.5 | 29.8 | 12.3 | 0.13 | 11.1 | 0.013 |
| 17–18 | 24.1 | 22.9 | 67.3 | 65.4 | 29.7 | 12.4 | 0.15 | 10.7 | 0.016 |
| 18–19 | 29.9 | 20.3 | 76.8 | 63.4 | 29.6 | 12.2 | 0.14 | 11.3 | 0.015 |
| 19–20 | 26 | 21 | 73.2 | 64.3 | 29.7 | 12.3 | 0.12 | 10.2 | 0.016 |
| 20–21 | 28.2 | 23 | 80.1 | 63.4 | 30.4 | 12.5 | 0.14 | 11 | 0.015 |
| 21–22 | 37.8 | 23.6 | 87.3 | 63.5 | 29.9 | 12.1 | 0.16 | 11.4 | 0.013 |
| 22–23 | 25.5 | 21.3 | 68.7 | 64.4 | 29.7 | 12.1 | 0.15 | 12 | 0.012 |
| 23–24 | 25.6 | 23.4 | 73 | 63 | 29.8 | 12.3 | 0.14 | 11.6 | 0.012 |
| 24–25 | 33.8 | 23.6 | 73.2 | 62.6 | 29 | 11.8 | 0.15 | 11.4 | 0.015 |
| 25–26 | 26.4 | 29.5 | 67.1 | 64.1 | 29.4 | 12 | 0.1 | 11 | 0.014 |
| 26–27 | 25.4 | 22.1 | 65.6 | 63.6 | 29.4 | 12.1 | 0.14 | 11.1 | 0.012 |
| 27–28 | 28.3 | 18.8 | 69.2 | 62.9 | 28.8 | 11.9 | 0.12 | 11.3 | 0.013 |
| 28–29 | 26.4 | 22.3 | 76.8 | 63.5 | 30 | 12.3 | 0.13 | 11.7 | 0.013 |
| 29–30 | 27.7 | 20 | 72.4 | 62.6 | 29.4 | 12.2 | 0.12 | 10.6 | 0.014 |
| Mean | 27.97 | 24.24 | 77.87 | 64.63 | 30.21 | 12.13 | 0.15 | 11.24 | 0.02 |
| STD | 2.91 | 4.11 | 11.85 | 1.37 | 1.63 | 0.27 | 0.04 | 0.62 | 0.01 |
| Median | 27.55 | 22.95 | 74.3 | 64.45 | 29.7 | 12.2 | 0.14 | 11.3 | 0.015 |
| MAD | 1.55 | 1.8 | 4.3 | 1.05 | 0.4 | 0.15 | 0.02 | 0.45 | 0.002 |

in order of Zn > Cr > Ni > Cu > Pb > Co > As > Cd > Hg in their concentrations. The concentrations of Zn and Cr are found maximum for both sites varying in between 65–102 µg g$^{-1}$ (S4), 65.6–123 µg g$^{-1}$ (S5), and 61.2–71.5 µg g$^{-1}$ (S4), and 62.6–67.6 µg g$^{-1}$ (S5), respectively, while minimum concentrations are observed for Hg with value in the range of 0.012–0.046 µg g$^{-1}$ and 0.012–0.039 µg g$^{-1}$ followed by Cd having value in the range of 0.12–0.24 µg g$^{-1}$ and 0.10–0.25 µg g$^{-1}$ for sites S4 and S5 respectively. Relatively higher concentration and small variability are observed for Zn, Cr, and Pb suggesting that they may be influenced by similar kinds of anthropogenic emission factors. The figure clearly reflects the similar variation of heavy metals with respect to time for both the sites S4 and S5, having an increasing trend for Zn, Ni, and Pb (Fig. 3(a–c)). A sharp increase in these three elements is observed in the early 1990s and reached a peak value in 2011 that may be associated with the rapid economic development, urbanization, and population expansion which cause a large consumption of fossil fuels and energy demands. Similar results are also observed by Kang et al. (2018) in the sediments of Jiaozhou Bay while Sun et al. (2019) found that the anthropogenic activities cause the higher concentration of heavy metals in the sediments of Yangtze River Estuary and the East China Sea. On the other hand, a large fluctuation in trend is observed for Cr, Cd, and Cu (Fig. 3(d–f)) which reached a peak value in 1980 suggesting

towards the intensification in industrial waste and smelter emissions from the industries. After that, a negative trend can be easily seen in Fig. 3 (d–f) for all the three elements at both the sites having different "z" values which are mainly because of the different industrial emission control policies implemented by the State Development Planning Commission. After 2000, a sharp increasing trend in Cd is also observed at both the sites S4 and S5, suggesting the enhancement in chemical industries near the sites. Apart from this, the concentration of the rest of the three trace elements, i.e., Co, As, and Hg, shows an overall decreasing trend at both sites S4 and S5 (Fig. 3 (g - i)). A sharp decrease in the trend of Co and As is observed after the year 2000 while for Hg, it is in since early 1940 which may be due to emission control policies from the government for the mitigation of hazardous materials (e.g., Hg and As).

## Potential emission sources of heavy metals

The correlation among the heavy metals may reflect the common emission source and migration of these metals (Islam et al. 2018; Kükrer et al. 2014). In order to investigate the common emission sources of the heavy metals in sediments, the Pearson's correlation analysis has been performed and the correlations among the heavy metals at both sites are given in Table 5. The concentration of Cu, Cr, Ni, and Co at site S4 and Pb, Zn, Ni, Cr, and Hg at site S5 showed a strong correlation to each other indicating the probably common emission sources (Liu et al. 2019; Sun et al. 2018). However, the concentration of other metals at both the sites S4 and S5 showed a negative or poor correlation to each other suggesting their different emission sources (Zhang et al. 2019; Sun et al. 2018). In addition, the PMF model has been also performed and three major emission factors which are viz. coal combustion, manufacturing, and smelting dust are identified. The percentage factor profiles and the concentration of PMF estimated factors of each heavy metal are given in Fig. 4. Factor 1 (i.e., coal combustion) is largely considered by Pb, Zn, and Ni with their fractional contribution of nearly 79%, 67%, and 19% respectively. The second factor (i.e., manufacturing) is mainly dominated by the Cr, Ni, and Co having their fractional contribution nearly 87%, 72%, and 65% respectively. Apart from this, factor 3 (i.e., smelting dust) is mainly associated

**Fig. 3** Time trends of concentrations ($\mu g g^{-1}$) of Zn (a), Ni (b), Pb (c), Cr (d), Cd (e), Cu (f), Co (g), As (h), and Hg (i). The lines in black color were based on the data of metals in S4; the lines in red color were based on the data of metals in S5
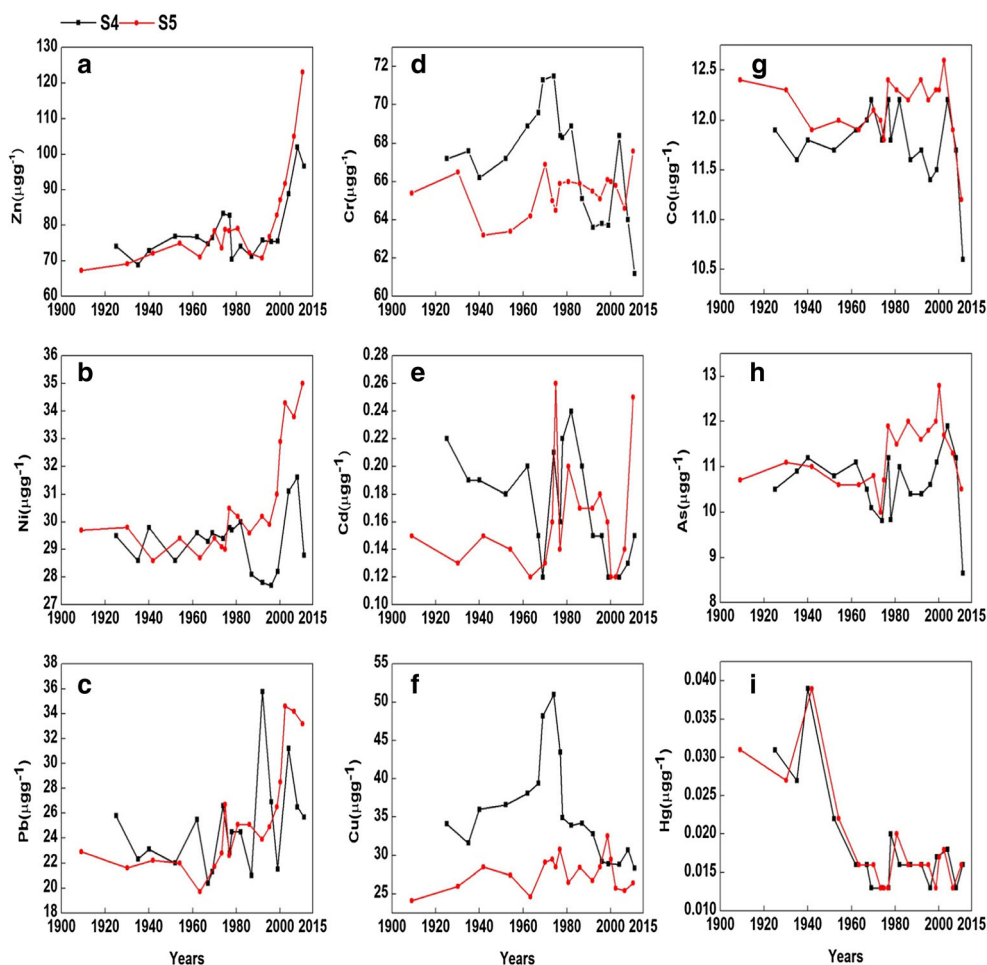
**Table 5** Correlation matrix between different heavy metals at core site S4 and S5

| S4 | Cu | Pb | Zn | Cr | Ni | Co | Cd | As | Hg |
|----|----|----|----|----|----|----|----|----|----|
| Cu | 1.00 | | | | | | | | |
| Pb | − 0.038 | 1.00 | | | | | | | |
| Zn | 0.121 | 0.453* | 1.00 | | | | | | |
| Cr | *0.757** | 0.015 | − 0.065** | 1.00 | | | | | |
| Ni | 0.273 | 0.287 | *0.597* | 0.401* | 1.00 | | | | |
| Co | 0.477** | 0.16 | 0.041 | *0.642** | *0.674** | 1.00 | | | |
| Cd | 0.23 | 0.12 | − 0.207 | 0.344 | 0.124 | 0.201** | 1.00 | | |
| As | − 0.012 | 0.07 | 0.088 | 0.144 | *0.525** | *0.698* | − 0.101 | 1.00 | |
| Hg | − 0.033 | 0.038 | 0.196 | 0.103 | 0.204 | − 0.004 | 0.089 | 0.059 | 1.00 |

| S5 | Cu | Pb | Zn | Cr | Ni | Co | Cd | As | Hg |
|----|----|----|----|----|----|----|----|----|----|
| Cu | 1.00 | | | | | | | | |
| Pb | − 0.091 | 1.00 | | | | | | | |
| Zn | 0.101 | *0.741** | 1.00 | | | | | | |
| Cr | − 0.127 | 0.453* | 0.431* | 1.00 | | | | | |
| Ni | − 0.133 | *0.841** | *0.867** | *0.521** | 1.00 | | | | |
| Co | − 0.067 | − 0.172 | − 0.409* | 0.023 | − 0.071 | 1.00 | | | |
| Cd | 0.108 | 0.291 | 0.427* | 0.35 | 0.177 | − 0.461* | 1.00 | | |
| As | 0.222 | 0.2156 | 0.4 | 0.159 | 0.267 | 0.397* | − 0.101 | 1.00 | |
| Hg | − 0.119 | *0.786** | *0.754** | 0.412* | *0.858** | − 0.121 | 0.118 | 0.407 | 1.00 |

Significant correlations are shown in italics

*Significant at $p < 0.05$ levels

**Significant at $p < 0.01$ levels

with Cd, Zn, and Cr with their contribution 75%, 33%, and 29% respectively. Earlier studies also suggest that coal combustion (Bing et al. 2019), waste incineration (Wang et al. 2019), agricultural sources (Huang et al. 2018), and steel smelting (Zhang et al. 2018) are the major sources of Zn into the environment. During the last three decades, the rapid development of economy in NCP causes a large consumption of coal and oil to fulfill energy demands resulting to the increasing trend of Zn into the atmosphere which is also clearly reflected in Fig. 3 (a). Coal and leaded gasoline combustion are the major emission sources of Pb (Jingchun et al. 2012). The emission from steel, plastic, and paint production and their wastewater discharge are also found to be the main contributors of the Pb. Earlier studies reported that Cr and Ni are abundant in anthropogenic waste, including sewage sludge and wastewater (Liu et al. 2019; Dwivedi and Vankar 2014; Li et al. 2014). Studies also suggest that As and Cd mainly come from the industrial wastewater such as chemical industry waste, electroplating, mining, and refining processes (Liu et al. 2019; Oliveira Zoffoli et al. 2013; Tian et al. 2010). Cu mainly comes from the metal smelting industries and printed circuit board industries (Chen et al. 2012), while Co is widely used in magnetic materials and emitted from the stainless steel, alloys, and batteries industries (Islam et al. 2018).

There are a large population (over 13 million) and a number of industries/factories in the Tianjin region and hence is attributed to the emission sources of heavy metals. Based on the results of the source resolution of the PMF model, emission from manufacturing have the maximum contribution (40%) to the total heavy metals in sediments followed by the coal consumption (32%) and smelting dust (28%) (Fig. 5), which attributed to higher concentration of Pb, Cr, Ni, and Zn respectively (Bozkurt et al. 2018; Liu et al. 2017; Belis et al. 2013). A relatively larger fraction of heavy metals from manufacturing is mainly because of Tianjin Nangang Industrial Park, which focuses on the development of petrochemical industry, port logistics industry, and metallurgical equipment manufacturing industry (Lu 2016).

## Impacts of local emissions on heavy metal loadings

The core sites are surrounded by a large number of industries mainly from the petrochemicals, oils, and steel plants which emit tons of hazardous environmental pollutants into the atmosphere and cause several complications. Figure 6 shows the trend of major heavy metals at both the core sites S4 and S5 (Fig. 6a and b) and consumption of coal and crude oil (Fig. 6c) in Tianjin province. The figure reflects that during the mid-

**Fig. 4** PMF source factors of coal, manufacturing, and smelting dust for S4 and S5
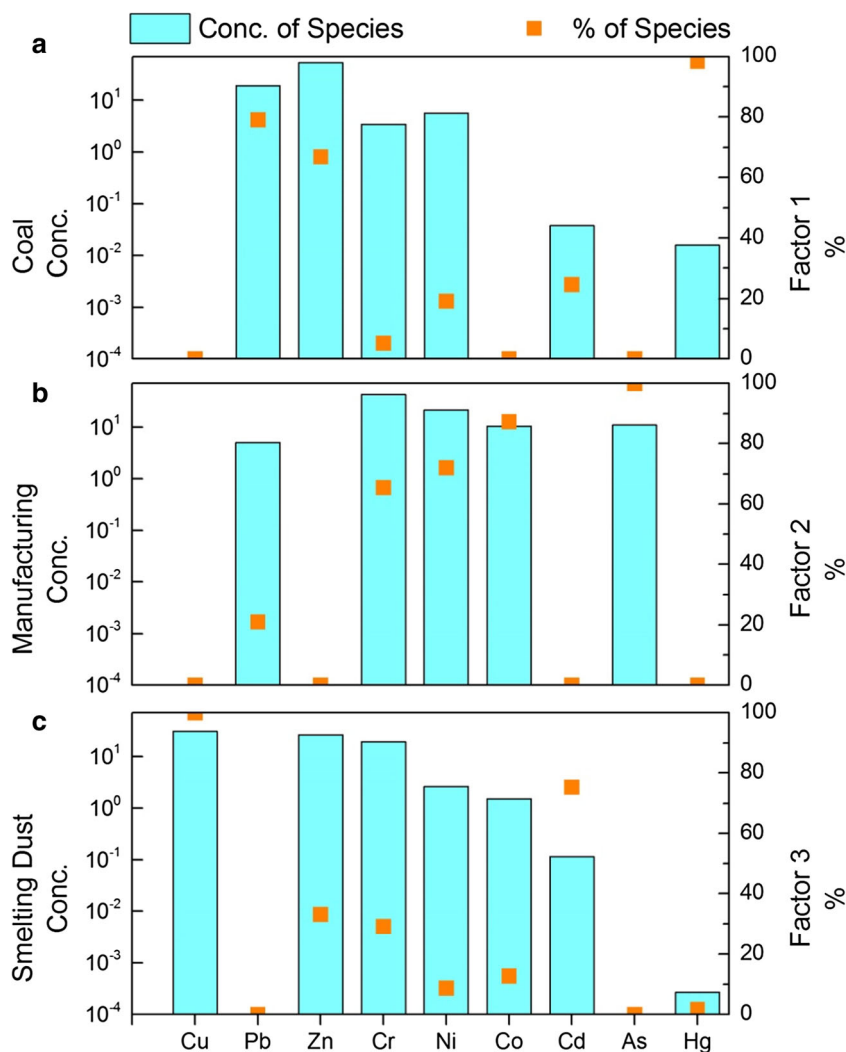


twentieth century, the concentration of Zn, Cr, Cu, and Pb at both sites increased which is more prominent after 1964 mainly
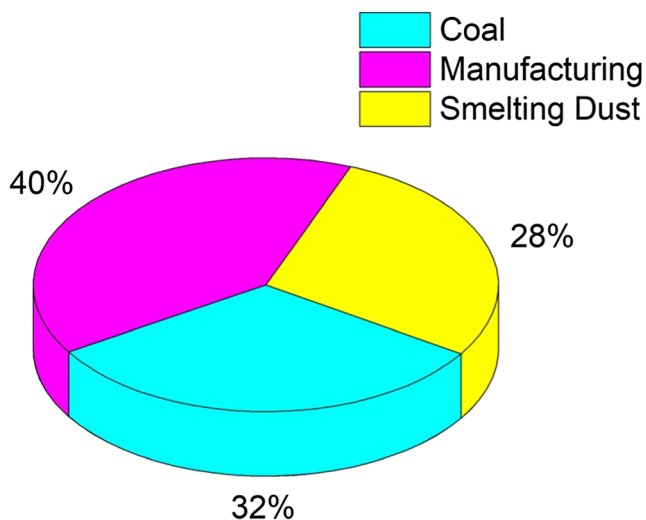


**Fig. 5** Relative contributions of coal, manufacturing, and smelting dust for both core sites S4 and S5

attributed to the opening of Dagang Oilfield (Fig. 6a and b) and injected plenty of heavy metals into the atmosphere. The sharp increase in Cu, Zn, and Pb, in contrast to the relatively smaller increase in Cr concentrations, suggests that the opening of Dagang Oilfield affects Cu, Zn, and Pb loadings more strongly than Cr loadings which also reflect by relatively larger consumption of crude oil than coal (Fig. 6c). Earlier studies also suggest that oil field development can lead to the enhancement in heavy metal concentration (Xiaowen et al. 2015; Liu 2015). A higher concentration of few heavy metals, i.e., Zn (288.7 $\mu g\,g^{-1}$), Pb (66.1 $\mu g\,g^{-1}$), Cu (22.7 $\mu g\,g^{-1}$), Ni (15.3 $\mu g\,g^{-1}$), and Cd (3.1 $\mu g\,g^{-1}$), is reported for oily sludge (John 2013). Rong et al. (2015) also found multiple heavy metals, i.e., Zn, Cd, Pb, Cu, As, and Hg, in drilling solid waste having their concentrations 1803, 62.1, 37.2, 25.5, 3.2, and 0.14 $\mu g\,g^{-1}$, respectively. However, the concentration of Ni, Co, and As is mostly unaffected by the Dagang Oilfield suggesting towards small amount emission of these heavy metals from the oil industry. After the late 1970s, the concentration of these heavy metals decreases (Fig. 6a and b) that may be mainly because of changes in electricity generation and

**Fig. 6** Time trends of heavy metals in S4 (**a**) and S5 (**b**); and coal and crude oil consumption in Tianjin (**c**) (https://www.doc88.com/p-0911392153730.html)
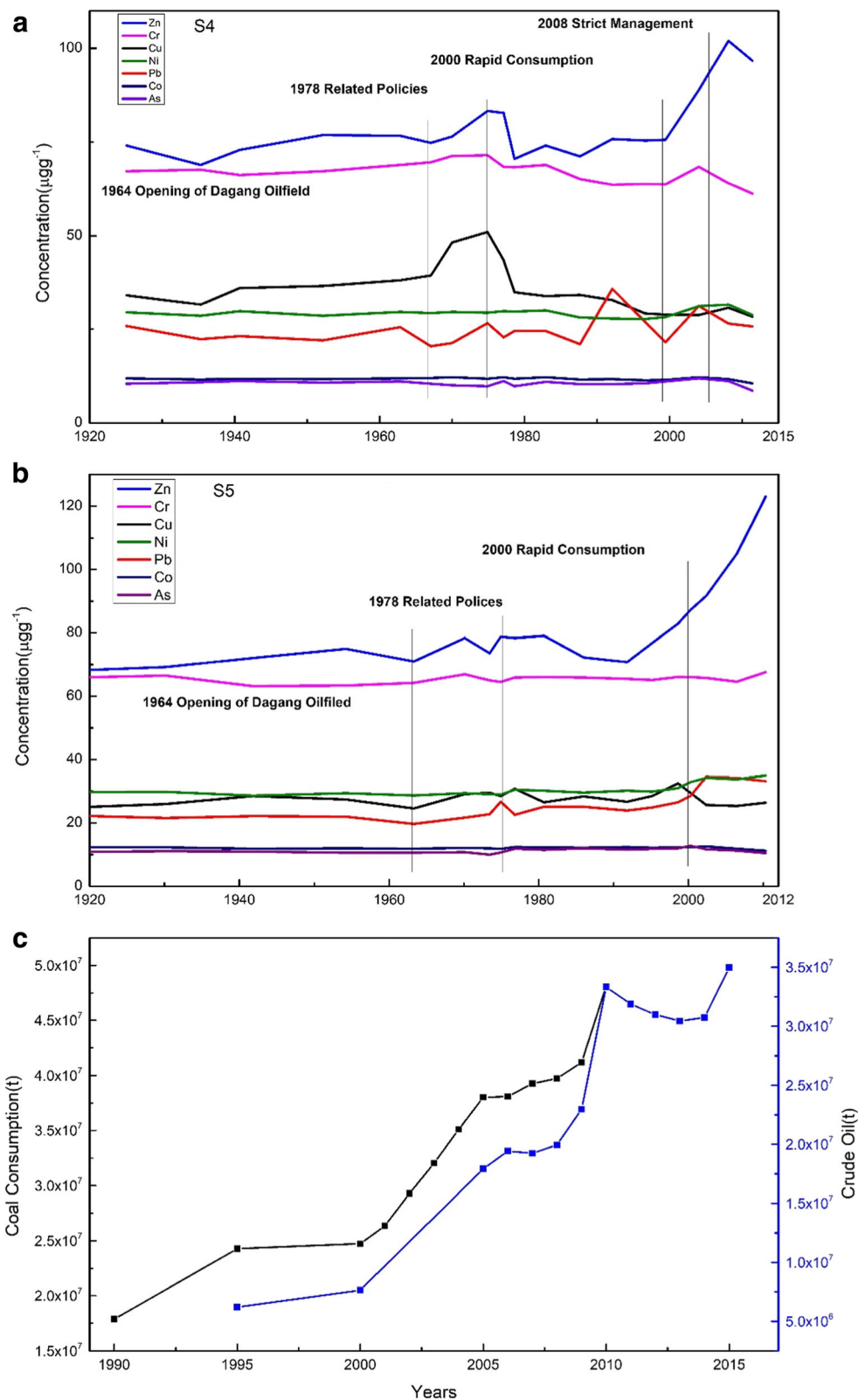


different environmental legislative laws. In 1978, the State Development Planning Commission, the State Economic Commission, and the leading group for environmental protection

under the State Council jointly formulated the first list of key industrial and mining enterprises in China to mitigate the serious environmental pollution within a time limit (Hongchun 2009). A

**Table 6** Laws and regulations carried out in 2013 and 2014 (https://wenku.baidu.com/view/f3b2dcbf2cc58bd63086bd53.html)

| Pollution prevention | Energy conservation |
| --- | --- |
| 2013.5 Cement industry pollution prevention technology policy | 2013.5 Guideline for accelerating the development of green recycling and low-carbon transportation |
| 2013.5 Steel industry pollution prevention and control technology policy | 2013.8 Opinions on accelerating the development of energy conservation and environmental protection industries |
| 2013.5 Sulfuric acid industrial pollution prevention and control technology policy | 2014.7 Guidance on accelerating the promotion and application of new energy vehicles |
| 2013.5 Volatile organic pollution control technology policy | 2014.8 New production of environmental protection standards for motor vehicles |
| 2013.9 Town drainage and sewage treatment regulations | 2014.9 New energy vehicle promotion work plan for public service areas such as Beijing-Tianjin-Hebei bus |

sharp increase in Zn after the 1990s is mainly attributed to the higher consumption of coal and crude oil which is more intense after the year 2000 (Fig. 6a and b) and can be easily seen in Fig. 6 c. A decreasing trend in heavy metals (mainly in Zn) is observed in 2013 which may be mainly due to the changes in power consumption method, i.e., from "coal to gas" and "coal in electricity," causing a reduction in heavy metal pollution along with a series of different laws and regulations focusing on environmental protection (Table 6). In addition, rapid increase during 2005–2010 may be also associated with the large consumption of coal from the major provinces adjacent to the studied area (Shandong, Hebei, Tianjin, and Beijing). A large number of heavy metal pollutants are reported through the coal consumption with the order of Pb > Cd > Zn > Ni > Co > Cu in their concentration (Yong et al. 2007).

## Risk assessment of heavy metals

Characterizing heavy metal contamination is also essential for effective ecosystem management, as the remobilization of heavy metal poses a serious threat to both the ecosystem and human health. To assess the potential risk of the heavy metal contamination present in sediments, the risk assessment analysis is performed. Since heavy metals in sediments always occur as

**Table 7** The metal guideline values of some different criteria used to distinguish sediment quality ($\mu g\ g^{-1}$)

|  | Cd | Cr | Cu | Ni | Pb | Zn | As | Hg |
| --- | --- | --- | --- | --- | --- | --- | --- | --- |
| Target[a] | 0.4 | 25 | 20 | 20 | 35 | 75 |  | 0.2 |
| Trigger[b] | 1.0 | 50 | 55 | 35 | 65 | 150 |  | 0.8 |
| Action[c] | 1.5 | 80 | 65 | 40 | 75 | 200 |  | 1.0 |
| ERL | 1.2 | 81 | 34 | 20.9 | 47 | 150 | 8.2 | 0.15 |
| ERM | 9.6 | 370 | 270 | 51.6 | 218 | 410 | 70 | 0.71 |

[a] The desired quality for fairly clean sediment that is close to background levels

[b] The sediment is moderately contaminated

[c] Heavily polluted sediments

*ERL* effect range low (NOAA), *ERM* effect range medium (NOAA)

complex mixtures, the mean ERM quotient method has been applied to determine the possible biological effect of combined toxicant groups. It is a well-accepted and widely used tool to understand the toxic effects of the pollutants on living organisms in the polluted environment (Tunca et al. 2018; Li et al. 2016b; Long et al. 2000). Further details about this method are described elsewhere (Gao and Chen 2012). ERM guideline values indicate concentrations above which adverse effects on biota are frequently observed while effects range low (ERL) guideline values indicate concentrations below which adverse effects on biota are rarely observed. The mean ERM quotients' value less than 0.1 suggests a 9% probability of being toxic; the value in the range of 0.11–0.5 has a 21% probability of being toxic; and the value in between 0.51 and 1.5 has a 49% probability of being toxic while the mean ERM quotients of > 1.50 have a 76% probability of being toxic (Birch 2018; Tunca et al. 2018; Long et al. 2000). The calculated mean ERM quotients of S4 and S5 for all the eight studied metals (no previous ERM data of Co has been found) are found ∼ 0.17 for both sites, indicating the environment is relatively less toxic (i.e., nearly 21% probability of being toxic) and action for the mitigation is still needed. Sediment quality is based on a criterion given in Table 7 (Joy et al. 2019; Birch 2018; Tunca et al. 2018). The concentrations of Cr is found higher than trigger values (Table 7) which suggest the moderate contamination of sediments; however, the concentrations of Cu, Ni, and Zn are found higher than the target values, and lower than the trigger values. On the other hand, concentrations of Pb, Cd, and Hg found lower than target values indicate virtually no pollution in the sediments. Our results suggest that Ni and As exceeded the ERL guideline values, which is potentially harmful to the benthic organisms.

## Conclusion

The outcomes of the present study provide information about the characteristics of heavy metal pollution at two nearby salt marsh site close to Bohai Bay. The present study reveals that the overall sediment quality has been largely impacted by heavy metal concentrations. Results suggest that Zn and Cr

have maximum concentration among all the studied heavy metals. An overall increasing trend in heavy metal is found with significant fluctuation which is mainly associated with different anthropogenic emission sources, energy consumption methods, and environmental protection policies. PMF model suggests three major emission source sectors, i.e., coal combustion, manufacturing, and smelling dust, having their contribution of 32%, 40%, and 28% respectively to the total heavy metal burden. Results also suggest that Cr, Ni, and Co mainly originated from the industrial sources and Cd mainly originated from the smelting dust; however, coal combustion is found to be the major source of Pb. The observed mean ERM quotients in this study indicate that the combination of the eight studied metals might be relatively less toxic (21% probability of being toxic), and this situation should be mitigated by related policies and regulations. Historical reconstruction of heavy metal pollution demonstrates that while modern heavy metal loading is substantial, the historical heavy metal loading can be significantly larger. This study also reveals that control in heavy metal emissions from the industries through different environmental policies could be quickly lost due to the establishment of other industries. For example, in the late 1970s, concentrations of heavy metals decreased as a result of related policies being established, but this trend did not last very long; in the late 1990s, it bounced back due to other industries. Thus, with the rapid increase in industrialization and economic development in this region, additional consideration should be paid and effective environmental policies and legislative laws in long-term future perspective are highly needed.

## References

Belis CA, Karagulian F, Larsen BR, Hopke PK (2013) Critical review and meta-analysis of ambient particulate matter source apportionment using receptor models in Europe. Atmos Environ 69:94–108

Bing H, Wu Y, Zhou J, Sun H, Wang X, Zhu H (2019) Spatial variation of heavy metal contamination in the riparian sediments after two-year flow regulation in the Three Gorges Reservoir, China. Sci Total Environ 649:1004–1016

Birch GF (2018) A review of chemical-based sediment quality assessment methodologies for the marine environment. Mar Pollut Bull 133:218–232

Bozkurt Z, Gaga EO, Taşpınar F, Arı A, Pekey B, Pekey H, Döğeroğlu T, Üzmez ÖÖ (2018) Atmospheric ambient trace element concentrations of PM10 at urban and sub-urban sites: source apportionment and health risk estimation. Environ Monit Assess 190:168

Carslaw DC (2005) Evidence of an increasing NO/NOX emissions ratio from road traffic emissions. Atmos Environ 39:4793–4802

Chen TR, Yu KF, Li S, Price GJ, Shi Q, Wei GJ (2010) Heavy metal pollution recorded in Porites corals from Daya Bay, northern South China Sea. Mar Environ Res 70:318–326

Chen X, Lu X, Yang G (2012) Sources identification of heavy metals in urban topsoil from inside the Xian Second Ring road, NW China using multivariate statistical methods. Catena 98:73–78

Chen J, Han T, Li X, He X, Wang Y, Chen F, Song X, Zhou D, Wang X (2018) Occurrence and distribution of marine natural organic pollutants: lipophilic marine algal toxins in the Yellow Sea and the Bohai Sea, China. Sci Total Environ 612:931–939

Cong ZY, Kang SC, Gao SP, Zhang YL, Li Q, Kawamura K (2013) Historical trends of atmospheric black carbon on Tibetan Plateau as reconstructed from a 150-year lake sediment record. Environ Sci Technol 47:2579–2586

Dai L, Wang L, Liang T, Zhang Y, Li J, Xiao J, Dong L, Zhang H (2019) Geostatistical analyses and co-occurrence correlations of heavy metals distribution with various types of land use within a watershed in eastern QingHai-Tibet Plateau, China. Sci Total Environ 653: 849–859

Duan J, Tan J (2013) Atmospheric heavy metals and Arsenic in China: Situation, sources and control policies. Atmos Environ 74:93–101

Dwivedi AK, Vankar PS (2014) Source identification study of heavy metal contamination in the industrial hub of Unnao, India Environ. Monit Assess 186:3531–3539

Fang TH, Chen RY (2010) Mercury contamination and accumulation in sediments of the East China Sea. J Environ Sci 22:1164–1170

Fang Y, Chen Y, Tian C, Lin T, Hu L, Huang G, Tang J, Li J, Zhang G (2015) Flux and budget of bc in the continental shelf seas adjacent to chinese high bc emission source regions. Glob Biogeochem Cycles 29(7):957–972

Fang Y, Chen Y, Tian C, Lin T, Hu L, Li J, Zhang G (2016) Application of PMF receptor model merging with PAHs signatures for source apportionment of black carbon in the continental shelf surface sediments of the Bohai and yellow seas, China. J Geophys Res Oceans 121:1346–1359

Fang Y, Chen Y, Tian C, Wang X, Lin T, Hu L, Li J, Zhang G, Luo Y (2018) Cycling and budgets of organic and black carbon in coastal Bohai Sea, China: Impacts of natural and anthropogenic perturbations. Glob Biogeochem Cycles 32:971–986

Feng WL, Guo ZH, Peng C, Xiao XY, Shi L, Han XQ (2018) Modelling mass balance of cadmium in paddy soils under long term control scenarios. Environ Sci: Processes Impacts 20:1158–1166

Gao X, Chen CT (2012) Heavy metal pollution status in surface sediments of the coastal Bohai Bay. Water Res 46:1901–1911

Gao X, Li P, Chen CTA (2013) Assessment of sediment quality in two important areas of mariculture in the bohai sea and the northern yellow sea based on acid-volatile sulfide and simultaneously extracted metal results. Mar Pollut Bull 72(1):281–288

Gao, C.A., Lin, Q.X., Zhang, S.Q., He, J.B., Lu, X.G., Wang, G.P. (2014) Historical trends of atmospheric black carbon on Sanjiang Plain as reconstructed from a 150-year peat record. Scientific Reports 4.

Gao JJ, Shi HH, Dai ZJ, Mei XF, Zong HB, Yang HW, Hu LL, Li SS (2018) Linkages between the spatial toxicity of sediments and sediment dynamics in the Yangtze River Estuary and neighboring East China Sea. Environ Pollut 233:1138–1146

Ghosh SP, Maiti SK (2018) Evaluation of heavy metal contamination in roadside deposited sediments and road surface runoff: a case study. Environ Earth Sci 77:267

Grigholm B, Mayewski PA, Aizen V, Kreutz K, Wake CP, Aizen E, Kang S, Maasch KA, Handley MJ, Sneed SB (2016) Mid-twentieth century increases in anthropogenic Pb, Cd and Cu in central Asia set in hemispheric perspective using Tien Shan ice core. Atmos Environ 131:17–28

Gusiatin ZM, Kulikowska D (2014) The usability of the IR, RAC and MRI indices of heavy metal distribution to assess the environmental quality of sewage sludge composts. Waste Manag 34:1227–1236

Han YM (2015) Elemental carbon and polycyclic aromatic compounds in a 150-year sediment core from lake qinghai, tibetan plateau, china: influence of regional and local sources and transport pathways. Environ Sci Technol 7(49):4176–4183

Han YM, Cao JJ, Yan BZ, Kenna TC, Jin ZD, Cheng Y (2011) Comparison of elemental carbon in lake sediments measured by three different methods and 150-year pollution history in eastern china. Environ Sci Technol 45(12):5287–5293

He Z, Li F, Dominech S, Wen X, Yang S (2019) Heavy metals of surface sediments in the Changjiang (Yangtze River) Estuary: distribution, speciation and environmental risks. J Geochem Explor 198:18–28

Hirsch RM, Slack JR, Smith RA (1982) Techniques of trend analysis for monthly water quality data. Water Resour Res 18:107–121

Hoang GM, Fujiwara T, Pham, Phu. TS., Nguyen, L.D. (2018) Sustainable solid waste management system using multi-objective decision-making model: a method for maximizing social acceptance in Hoi An city, Vietnam. Environ Sci Pollut Res

Hongchun, Z. (2009) Evolution of Environmental Protection Policy in China during the past 30 years of reform and opening up. Journal of Nanjing University (philosophy, Humanities, Social Sciences) 46: 31-40.

Hopke PK (1991) An introduction to receptor modeling. Chemom Intell Lab Syst 10:21–43

Hu B, Shao S, Fu Z, Li Y, Ni H, Chen S, Zhou Y, Jin B, Shi Z (2019) Identifying heavy metal pollution hot spots in soil-rice systems: a case study in South of Yangtze River Delta, China. Sci Total Environ 658:614–625

Huang J, Guo S, Zeng GM, Li F, Gu Y, Shi Y, Peng S (2018) A new exploration of health risk assessment quantification from sources of soil heavy metals under different land use. Environ Pollut 243:49–58

Islam MS, Hossain MB, Matin A, Sarker Md SI (2018) Assessment of heavy metal pollution, distribution and source apportionment in the sediment from Feni River estuary, Bangladesh. Chemosphere 202: 25–32

Jaiswal RK, Lohani AK, Tiwari HL (2015) Statistical analysis for change detection and trend assessment in climatological parameters. Environ Processes 2(4):729–749

Ji CX, Yang GP, Chen Y, Zhang PY (2019) Distribution, degradation and bioavailability of dissolved organic matter in the East China Sea. Biogeochemistry 142(2):189–207

Jingchun D, Jihua S, Wang J, Fahe C (2012) Size distributions and sources of elements in particulate matter at curbside, urban and rural sites in Beijing. J Environ Sci 24:87–94

John NM (2013) Heavy metals content of crude oil sludge/poultry manure and crude oil sludge/municipal solid waste composts. Agric J

Jordanova M, Hristovski-Musa S, Violeta M, Katerina B, Suzana R, Melovski DKL (2018) Accumulation of heavy metals in some organs in Barbel and chub from Crn Drim River in the Republic of Macedonia. Bull Environ Contam Toxicol 3:392–397

Joy A, Anoop PP, Rajesh R, Mathew J, Mathew A, Gopinath A (2019) Spatial variation of trace element concentration and contamination assessment in the coral reef sediments of Lakshadweep Archipelago. Indian Ocean Mar Pollut Bull 146:106–116

Kang X, Song X, Yuan H, Li X, Li N, Duan L (2018) Historical trends of anthropogenic metals in sediments of Jiaozhou Bay over the last century. Mar Pollut Bull 135:176–182

Kara M, Hopke PK, Dumanoglu Y, Altiok H, Elbir T, Odabasi M, Bayram A (2015) Characterization of PM using multiple site data in a heavily industrialized region of Turkey. Aerosol Air Qual Res 15:11–27

Keshavarzi A, Kumar V (2018) Ecological risk assessment and source apportionment of heavy metal contamination in agricultural soils of Northeastern Iran. Int J Environ Health Res:1–17

Khaiwal R, Mor S (2019) Distribution and health risk assessment of arsenic and selected heavy metals in Groundwater of Chandigarh, India. Environ Pollut 250:820–830

Kükrer S, Seker S, Abaci ZT, Kutlu B (2014) Ecological risk assessment of heavy metals in surface sediments of northern littoral zone of Lake Çildir, Ardahan, Turkey. Environ Monit Assess 186(6): 3847–3857

Kumar B, Singh UK (2018) Source apportionment of heavy metals and their ecological risk in a tropical river basin system. Environ Sci Pollut Res 25(25):25443–25457

Li X, Wai OWH, Li YS, Coles BJ, Ramsey MH, Thornton I (2000) Heavy metal distribution in sediment profiles of the Pearl River estuary, South China. Appl Geochem 15:567–581

Li Z, Ma Z, van der Kuijp TJ, Yuan Z, Huang L (2014) A review of soil heavy metal pollution from mines in China: pollution and health risk assessment. Sci. Total Environ 468:843–853

Li L, Cui J, Liu J, Gao J, Bai Y, Shi X (2016a) Extensive study of potential harmful elements (Ag, As, Hg, Sb, and Se) in surface sediments of the Bohai Sea, China: Sources and environmental risks. Environ Pollut 219:432–439

Li H, Wang Q, Shao M, Wang J, Wang C, Sun Y, Qian X, Wu H, Yang M, Li F (2016b) Fractionation of airborne particulate-bound elements in haze-fog episode and associated health risks in a megacity of southeast China. Environ Pollut 208:655–662

Li JW, Chen B, Campa AMSDL, Alastuey A, Querol X, Rosa JDDL (2018) 2005-2014 trends of PM10 source contributions in an industrialized area of southern Spain ☆. Environ Pollut 236:570–579

Liang J, Feng C, Zeng G, Gao X, Zhong M, Li X, Li X, He X, Fang Y (2017) Spatial distribution and source identification of heavy metals in surface soils in a typical coal mine city, Lianyuan, China. Environ Pollut 225:681–690

Lin T, Hu L, Guo Z, Qin Y, Yang Z, Zhang G, Zheng M (2011) Sources of polycyclic aromatic hydrocarbons to sediments of the Bohai and Yellow Seas in East Asia. J Geophys Res 116

Lin Q, Liu E, Zhang E, Nath B, Shen J, Yuan H, Wang R (2017) Reconstruction of atmospheric trace metals pollution in Southwest China using sediments from a large and deep alpine lake: historical trends, sources and sediment focusing. Sci Total Environ 331:613–614

Liu X (2015) Pollution and environmental quality evaluation for soil in the oil production zones of an oil field. Environ Eng 33:126

Liu B, Wu J, Zhang J, Lu W, Yang J, Liang D, Dai Q, Bi X, Feng Y, Zhang Y (2017) Characterization and source apportionment of PM 2.5 based on error estimation from EPA PMF 5.0 model at a medium city in China. Environ Pollut 222:10–22

Liu Q, Jia J, Li S, Hu J (2019) Assessment of heavy metal pollution, distribution and quantitative source apportionment in surface sediments along a partially mixed estuary (Modaomen, China). Chemosphere 225:829–838

Long ER, Macdonald DD, Severn CG, Hong CB (2000) Classifying the probabilities of acute toxicity in marine sediments with empirically derived sediment quality guidelines Environ. Toxicol Chem 19(10): 2598–2601

Lu L (2016) The Tianjin Nangang industrial zone of the green house. China Business

Łuczyńska J, Paszczyk B, Łuczyński MJ (2018) Fish as a bioindicator of heavy metals pollution in aquatic ecosystem of Pluszne Lake, Poland, and risk assessment for consumer's health. Ecotoxicol Environ Saf 153:60–67

Macedo-Miranda G, Avila-Pérez P, Gil-Vargas P, Zarazúa G, Sánchez-Meza JC, Zepeda-Gómez C, Tejeda S (2016) Accumulation of heavy metals in mosses: a biomonitoring study. SpringerPlus 5: 715. https://doi.org/10.1186/s40064-016-2524-7

Maes T., Barry, J., Leslie, H.A., Vethaak A.D., Nicolaus E.E.M, Law R.J., Lyons B.P, Martinez R., Harley B., Thain, J.E. (2018) Below the surface: twenty-five years of seafloor litter monitoring in coastal seas of North West Europe (1992–2017). Sci Total Environ 630: 790–798.

Marchant BP, Saby NPA, Arrouays D (2017) A survey of topsoil arsenic and mercury concentrations across France. Chemosphere 181:635–644

Men C, Liu R, Xu F, Wang Q, Guo L, Shen Z (2018) Pollution characteristics, risk assessment, and source apportionment of heavy metals in road dust in Beijing. China Sci Total Environ 612:138–147

Montanher T, Neumaier A, Domes FJ, Glob Optim (2018) A computational study of global optimization solvers on two trust region sub-problems. J Glob Optim 71:915

Ming L, Dejiang F, Naishuang B, Xueshi S, Yuan T (2019) Impact of water-sediment regulation on the transport of heavy metals from the Yellow River to the sea in 2015. Sci Total Environ 658:268–279

Oliveira Zoffoli HJ, Brasil Do Amaral-Sobrinho NM, Zonta E, Luisi MV, Marcon G, Tolon-Becerra A (2013) Inputs of heavy metals due to agrochemical use in tobacco fields in Brazil's Southern Region. Environ Monit Assess 185:2423–2437

Peng H, Chen Y, Weng L, Ma J, Ma Y, Li Y, Islam Md. S (2019). Comparisons of heavy metal input inventory in agricultural soils in North and South China: A review. Sci Total Environ, 660:776–786.

Praveena SM, Ismail SNS, Aris AZ (2015) Health risk assessment of heavy metal exposure in urban soil from Seri Kembangan (Malaysia). Arab J Geosci 8:9753–9761

Rahman M, Dustegir M, Karim R, Haque A, Nicholls RJ, Darby SJ, Nakagawa H, Hossain M, Dunn FE, Akter M (2018) Recent sediment flux to the Ganges-Brahmaputra-Meghna delta system. Sci Total Environ 643:1054–1064

Ran Yl, Xing Wq, Liang S, Xiang Gq, Li Lp (2010) Heavy metal availability in soil near a lead smelter in the North China Plain. Asian J Ecotoxicol 5:592–598

Rong W, Ronghua W, Shihong C, Liping Q, Xiaojie X (2015) Analysis of heavy metals in drilling solid waste in a certain area. Oil and Gas Field Environ Protection 25:57–59

Song Q, Li J (2015) A review on human health consequences of metals exposure to e-waste in China. Environ Pollut 196:450–461

Sun XS, Fan DJ, Liu M, Tian Y, Pang Y, Liao HJ (2018) Source identification, geochemical normalization and influence factors of heavy metals in Yangtze River Estuary sediment. Environ Pollut 241:938–949

Sun C, Zhang Z, Cao H, Xu M, Xu L (2019) Concentrations, speciation, and ecological risk of heavy metals in the sediment of the Songhua River in an urban area with petrochemical industries. Chemosphere 219:538–545

Tan K, Liu X, Tang Q, Liu J, Yuan X, Yang Y (2011) Distribution regularity of heavy metals in North China Plain and its significance. Acta Geosci Sin 32:732–738

Tian HZ, Wang Y, Xue ZG, Cheng K, Qu YP, Chai FH, Hao JM (2010) Trend and characteristics of atmospheric emissions of Hg, As, and Se from coal combustion in China, 1980–2007. Atmos Chem Phys Discuss 10:20729–20768

Tian HZ, Zhu CY, Gao JJ, Cheng K, Hao JM, Wang K, Hua SB, Wang Y, Zhou JR (2015) Quantitative assessment of atmospheric emissions of toxic heavy metals from anthropogenic sources in China: historical trend, spatial distribution, uncertainties, and control policies. Atmos Chem Phys 15:10127–10147

Tunca E, Aydın M, Şahin ÜA (2018) An ecological risk investigation of marine sediment from the northern Mediterranean coasts (Aegean Sea) using multiple methods of pollution determination. Environ Sci Pollut Res 25:7487–7503

Wan D, Song L, Mao X, Yang J, Jin Z, Yang H (2019) One-century sediment records of heavy metal pollution on the southeast Mongolian Plateau: implications for air pollution trend in China. Chemosphere 220:539–545

Wang P, Hu Y, Cheng H (2019) Municipal solid waste (MSW) incineration fly ash as an important source of heavy metal pollution in China. Environ Pollut 252(A):461–475

Xiaowen F, Guanghong C, Jianguo C, Weizhong Q, Jianing W, Zhaojie C (2015) Analysis of pollution characteristics of heavy metals in soil of Shengli Oilfield. Shandong Sci 28:88–96

Yan F, Liu CL, Wei BW (2019) Evaluation of heavy metal pollution in the sediment of Poyang Lake based on stochastic geo-accumulation model (SGM). Sci Total Environ 659(1):1–6

Yin S, Wu Y, Xu W, Li Y, Shen Z, Feng C (2016) Contribution of the upper river, the estuarine region, and the adjacent sea to the heavy metal pollution in the Yangtze estuary. Chemosphere 155:564–572

Yong Y, Qiang Y, Qiang S, Shuiqing L, Hui W (2007) Contrastive study on PM10 speciation and heavy metal distribution in different coal combustion sources. Chin J Electr Eng 27:33–38

Zhang X, Zhong T, Liu L, Ouyang X (2015) Impact of soil heavy metal pollution on food safety in China. PLoS One 10(8):e0135182

Zhang Y, Han Y, Yang J, Zhu L, Zhong W (2017) Toxicities and risk assessment of heavy metals in sediments of Taihu Lake, China, based on sediment quality guide-lines. J Environ Sci 62:31–38

Zhang C, Shan B, Zhao Y, Song Z, Tang W (2018) Spatial distribution, fractionation, toxicity and risk assessment of surface sediments from the Baiyangdian Lake in northern China. Ecol Indic 90:633–642

Zhang M, He P, Qiao G, Huang J, Yuan X, Li Q (2019) Heavy metal contamination assessment of surface sediments of the Subei Shoal, China: Spatial distribution, source apportionment and ecological risk. Chemosphere 223:211–222

Zhou L, Liu G, Shen M, Hu R, Sun M, Liu Y (2019) Characteristics and health risk assessment of heavy metals in indoor dust from different functional areas in Hefei, China. Environ Pollut 251:841–849

Ziting L, Junqing Y, Baohua Z, Wei C, Lisha Z (2006) Application of burning loss analysis in the study of lake deposition and environmental change. Salt Lake Res 14:67–72